Received: 24 July 2019 | Revised: 15 February 2020 | Accepted: 5 March 2020

DOI: 10.1111/1440-1681.13300

CEPP Clinical and Experimental Pharmacology and Physiology WILEY

ORIGINAL ARTICLE

Diabetes and Obesity, Metabolic

Reduced store-operated Ca^{2+} entry impairs mesenteric artery function in response to high external glucose in type 2 diabetic ZDF rats

Christian Schach[1] | Michael Wester[1] | Florian Leibl[1] | Andreas Redel[2] | Michael Gruber[2] | Lars S. Maier[1] | Dierk Endemann[1] | Stefan Wagner[1]

[1]Abteilung für Kardiologie, Klinik und Poliklinik für Innere Medizin II, Universitäres Herzzentrum Regensburg, Universitätsklinikum Regensburg, Regensburg, Germany

[2]Klinik für Anästhesiologie, Universitäres Herzzentrum Regensburg, Universitätsklinikum Regensburg, Regensburg, Germany

Correspondence
Stefan Wagner, Abteilung für Kardiologie, Klinik und Poliklinik für Innere Medizin II, Universitäres Herzzentrum Regensburg, Universitätsklinikum Regensburg, Franz-Josef-Strauss-Allee 11, 93053 Regensburg, Germany.
Email: stefan.wagner@ukr.de

Funding information
The study was supported by individual funding of the first author within the ReForM B program of the University of Regensburg. SW is funded by DFG grants WA 2539/4-1, 5-1 and 7-1. LSM is funded by DFG grants MA 1982/5-1 and 7-1. SW and LSM are also funded by the DFG SFB 1350 grant (Project Number 387509280, TPA6), are supported by the ReForM C program of the faculty, and funded by the DZHK (Deutsches Zentrum für Herz-Kreislauf-Forschung; German Center for Cardiovascular Research).

Abstract

Diabetes is a major risk factor for cardiovascular disease, affecting both endothelial and smooth muscle cells. Store-operated Ca^{2+} channels (SOCCs) have been implicated in many diabetic complications. Vascular dysfunction is common in patients with diabetes, but the role of SOCCs in diabetic vasculopathy is still unclear. Our research aimed to investigate the effects of high glucose (HG) on store-operated Ca^{2+} entry (SOCE) in small arteries. Small mesenteric arteries from type 2 diabetic Zucker fatty rats (ZDF) versus their non-diabetic controls (Zucker lean, ZL) were examined in a pressurized myograph. Vascular smooth muscle cells (VSMC) were isolated and intracellular Ca^{2+} was measured (Fura 2-AM). A specific protocol to deplete intracellular Ca^{2+} stores and thereby open SOCCs, as well as pharmacological SOCE inhibitors (SKF-96365, BTP-2), were used to artificially activate and inhibit SOCE, respectively. High glucose (40 mmol/L) relaxed arteries in a SKF-sensitive manner. Diabetic arteries exhibited reduced HG-induced relaxation, as well as reduced contraction after Ca^{2+} replenishment. Further, the rise in intracellular Ca^{2+} on account of SOCE is diminished in diabetic versus non-diabetic VSMCs and was insensitive to HG in diabetic VSMCs. The expression of SOCC proteins was measured, detecting a downregulation of Orai1 in diabetes. In conclusion, diabetes leads to a reduction of SOCE and SOCE-induced contraction, which is unresponsive to HG-mediated inhibition. The reduced expression of Orai1 in diabetic arteries could account for the observed reduction in SOCE.

KEYWORDS

diabetes, high glucose, small mesenteric arteries, store-operated calcium entry, vascular smooth muscle, ZDF

1 | INTRODUCTION

Cardiovascular disease is the main cause of mortality and morbidity in diabetic patients, who have a two- to four-fold higher risk of cardiovascular events compared to individuals without diabetes.[1,2] This increased risk is generally attributed to the adverse effects of elevated blood glucose levels and oxidative stress, both of which can contribute to vascular damage and consequent cardiovascular complications.

The peer review history for this article is available at https://publons.com/publon/10.1111/cep.13300

Besides impaired endothelial function, vascular smooth muscle cell (VSMC) function is also altered in diabetic patients.[3] In VSMCs, intracellular Ca^{2+} is essential for activation of the contractile apparatus and is regulated by Ca^{2+} entry across the plasma membrane and Ca^{2+} release from internal stores. Transmembrane Ca^{2+} entry is controlled by either voltage-operated Ca^{2+} channels (LTCC) or receptor-operated Ca^{2+} channels.[4] Recent studies present evidence that store-operated Ca^{2+} entry (SOCE) may also play a vital role in replenishing intracellular Ca^{2+} stores and thereby increasing vascular contractility and tone.[5,6]

The molecular basis of SOCE involves at least two important proteins: stromal interaction molecule 1 (STIM1), which is localized to the membrane of the sarcoplasmic reticulum (SR), and the plasma membrane-localized Orai Ca^{2+} release-activated Ca^{2+} channel protein 1 (Orai1; for review see[7]).

The mechanisms of SOCE regulation in diabetic VSMCs are poorly understood. High extracellular glucose (HG) levels have been shown to relax VSMCs in non-diabetic subjects and animals in a variety of vascular beds, including mesenteric arteries.[8-10] Interestingly, the intestinal milieu during and after digestion is characterized by high luminal glucose concentration up to 50–100 mmol/L,[11] which may affect local blood flow.

Therefore, we tested whether SOCE-dependent regulation of the vascular tone of small mesenteric arteries (SMAs) is sensitive to high external glucose levels and whether this regulation is disturbed in a rat model of type 2 diabetes. We investigated Zucker diabetic fatty rats (ZDF), whose mesenteric arteries are known to exhibit reduced endothelium- or arachidonic acid-dependent relaxation, which has been shown to have pathological relevance in rodents and humans.[12-14] Here, we show that increased extracellular glucose levels inhibit SOCE, which results in SMA relaxation in non-diabetic lean control rats. Interestingly, we observed a reduced level of SOCE in the mesenteric arteries of ZDF rats that is possibly related to reduce STIM1-expression. In consequence, high extracellular glucose-dependent relaxation was dramatically blunted in SMAs of ZDF rats. This finding may be important for understanding the intestinal function of diabetic patients.

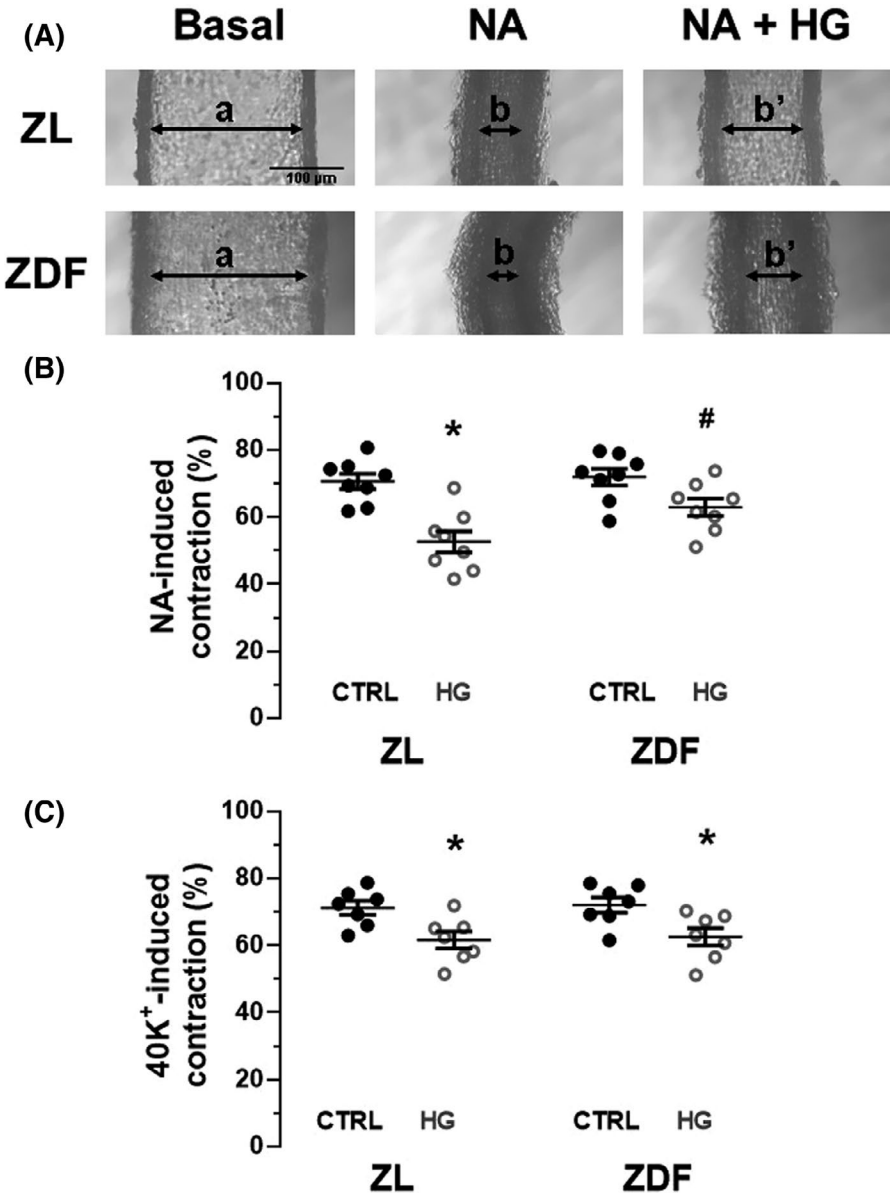

FIGURE 1 High glucose (HG)-dependent relaxation of rat small mesenteric arteries is impaired in Zucker diabetic fatty rats (ZDF). Small mesenteric arteries (SMA) mounted onto a pressurized myograph (55 mm Hg) were stimulated with a solution containing noradrenaline (NA, 10 µmol/L) or 40 mmol/L potassium ($40K^+$) in the presence or absence of high glucose (40 mmol/L glucose, HG). A, Representative myographic recordings of SMA diameters at rest (basal, left), precontracted with NA (middle, NA), and after addition of HG (right, NA + HG). Relative contraction was calculated as "(a-b)/a" with "a" representing the inner diameter at rest, "b" the inner diameter after contraction with NA and "b'" the inner diameter after contraction with NA in the presence of HG. Relative contractions are shown as scatter plots after NA- (B) or $40K^+$- (C) induced precontraction. Interestingly, exposure to HG resulted in vasorelaxation (ie less contraction) in SMAs of non-diabetic Zucker lean control rats (ZL) but not in SMAs of type 2 diabetic Zucker diabetic fatty rats (ZDF). $^*P < .05$ vs corresponding CTRL, $^{\#}P < .05$ vs corresponding ZL, two-way ANOVA, n = 7-8

2 | RESULTS

2.1 | High external glucose-dependent vascular relaxation is impaired in diabetes

Acute exposure to high extracellular glucose levels (HG) has been shown to relax the arteries of various vascular beds. To investigate the effect of HG on diabetic vessels, we measured the diameter of SMAs isolated from diabetic fatty rats (ZDF) and lean control rats (ZL) using a pressurized myograph. Compared to ZL, SMAs from ZDF rats showed no difference in agonist-induced or 40 mmol/L K^+ ($40K^+$)-induced contraction amplitude (Figure 1). Perfusion with noradrenaline (NA) reduced vessel diameters from 209 ± 11 to 62 ± 5 µm (ZL) vs from 215 ± 12 to 60 ± 6 µm (ZDF, n = 8, P = NS ZL vs ZDF). Exposure to $40K^+$ led to a mean reduction of vessel diameters from 207 ± 10 to 64 ± 5 µm (ZL) vs 216 ± 11 to 60 ± 6 µm (ZDF, n = 7, P = NS ZL vs ZDF). There was also no statistically significant difference between $40K^+$- and NA-induced diameter reduction. Interestingly, in ZL SMAs, exposure to high external glucose levels (HG, 40 mmol/L) resulted in a significant reduction of the NA-dependent contraction from 71 ± 3 to 53 ± 3% and also a reduction of the $40K^+$-dependent contraction from 72 ± 4 to 63 ± 4%, consistent with vascular relaxation (n = 8, $P < .05$ vs CTRL, Figure 1). In contrast, there was significantly less impairment of NA-dependent contraction by HG in SMAs of ZDF rats. Compared to CTRL, NA-dependent contractions were only reduced from 72 ± 3 to 62 ± 3% (n = 8, P = NS vs CTRL), which is significantly less than in ZL ($P < .05$ vs ZL + HG, Figure 1B) and could have implications for the function of diabetic mesenteric arteries under conditions of increased extracellular glucose levels. Notably, there was no difference in the impairment of $40K^+$-dependent contraction between ZL and ZDF in the presence of HG suggesting that the underlying mechanism involves a diabetes-dependent disruption of NA signalling. Removal of functional endothelium did not affect the differences observed between ZL and ZDF with respect to impairment of NA-dependent contraction in the presence of HG (Figure S1), suggesting that the endothelium is not involved.

2.2 | Intracellular Ca^{2+} handling is impaired in diabetic SMAs

The pharmacological SOCE inhibitors SKF-96365 (SKF; 10 µmol/L) and BTP-2 (BTP; 10 µmol/L) were used to test whether SOCE participates in NA-induced contractions. Exposure of SMAs to either SKF or BTP-2 significantly impaired NA-induced contraction in both ZL and ZDF rats (Figure 2A). However, for both SKF and BTP-2, this relaxing effect (i.e. impairment of NA-induced contraction) was significantly less pronounced in the SMAs of ZDF rats compared to ZL.

Simultaneous administration of either HG and SKF or HG and BTP resulted in no additional impairment of NA-dependent SMA

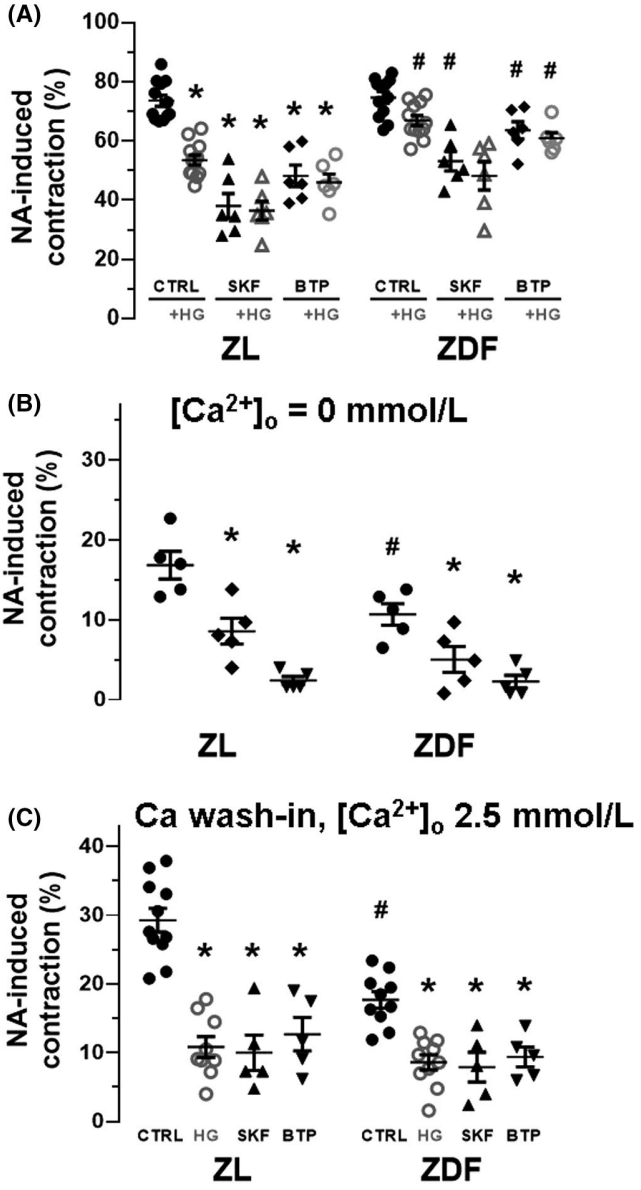

FIGURE 2 Zucker diabetic fatty rat (ZDF)-small mesenteric arteries (SMAs) display reduced store $[Ca^{2+}]$- and store-operated Ca^{2+} entry (SOCE)-dependent contraction. A, Scatter plots of noradrenaline (NA)-induced contractions (calculated as in Figure 1) for ZL and ZDF SMAs exposed to either high glucose (40 mmol/L, HG), the pharmacological SOCE inhibitors SKF-96365 (10 µmol/L, SKF) and BTP-2 (10 µmol/L, BTP), or a combination of HG and SOCE inhibitor (HG + SKF, HG + BTP). B, Scatter plots of NA-induced contractions upon repeated NA exposure in Ca^{2+} free solution as a measure of store $[Ca^{2+}]$-dependent contraction. Interestingly, store $[Ca^{2+}]$-dependent contraction (upon 1st NA exposure) was significantly reduced in SMAs of ZDF rats (vs ZL control). C, Scatter plots of SOCE-dependent NA-induced contractions after Ca^{2+} wash-in ($[Ca^{2+}]_o$ 2.5 mmol/L) and the addition of voltage-operated Ca2+ channels (LTCC) blocker nifedipine (1 µmol/L). Compared to ZL, the SOCE-dependent contraction was significantly impaired in SMAs of ZDF rats. This difference was blocked by exposure to HG, SKF or BTP. $^*P < .05$ vs corresponding CTRL, $^\#P < .05$ vs corresponding ZL, two-way ANOVA, n = 5-12. ● 1st NA-challenge; ◆: 2nd; ▼: 3rd

contraction in both ZL and ZDF, suggesting that high external glucose levels may impair NA-dependent contraction (i.e. induce relaxation) via SOCE inhibition.

To further investigate the mechanism underlying the impaired HG-dependent relaxation (after NA-dependent pre-contraction) in SMAs of ZDF compared to ZL rats, we investigated NA-dependent Ca^{2+} release from intracellular stores. Testing SMAs in a Ca^{2+}-free environment while simultaneously blocking LTCC with nifedipine (Nif, 1 µmol/L) can be used to measure the contraction elicited by exposure to NA when it exclusively depends upon intracellular Ca^{2+} release from the sarcoplasmic reticulum (SR). Consistent with this concept, repetitive exposures to NA resulted in complete emptying of SR Ca^{2+} content (and release) and rendered the SMAs unresponsive to a contraction stimulus. Figure 2B shows that after NA washout, contractions were progressively diminished upon each re-exposure to NA, consistent with emptying of SR Ca^{2+} stores. In this setting, the amplitude of the first NA-dependent contraction can be used as a measure of SR Ca^{2+} release. Interestingly, compared to ZL, the NA-dependent contraction in ZDF SMAs was significantly smaller (Figure 2B). The first NA exposure resulted in a relative contraction of 17 ± 3% in ZL, compared to only 11 ± 2% in ZDF SMAs (n = 5, $P < .05$ vs ZL), which supports the thesis that SR Ca^{2+} release is reduced in this model of type 2 diabetes.

After complete emptying of SR Ca^{2+} stores, switching to a Ca^{2+} containing (2.5 mmol/L) extracellular solution in the presence of Nif resulted in a tonic contraction consistent with SOCE-dependent myofilament activation (Figure 2C). Importantly, compared to ZL SMAs, this relative contraction was reduced in ZDF by 40% from 29 ± 3% to 17 ± 3% (n = 5-11, $P < .05$ vs ZL) suggesting that SOCE amplitude may be reduced in SMAs of rats with type 2 diabetes.

It has been previously shown that exposure to HG also inhibits SOCE.[15] Consistently, exposure to either HG or SOCE inhibitors (SKF or BTP-2) completely abolished the NA-dependent, Nif-insensitive contraction after Ca^{2+} replenishment (Figure 2C).

These results suggest that HG-dependent vascular relaxation (after NA-dependent pre-contraction) may be mediated through the inhibition of SOCE, which may also explain why diabetic SMAs with potentially reduced SOCE showed a less diminished contractile response in a HG environment.

In contrast to NA-induced SMA contraction, $40K^+$-dependent contraction is mediated by membrane depolarization and activation of L-type Ca^{2+} channels. Consistently, SKF had only a marginal inhibitory effect on $40K^+$-dependent contractions. SKF reduced $40K^+$-induced contraction from 71 ± 2% to 11 ± 1% in ZL (n = 6, P = NS) and from 69 ± 2% to 10 ± 1% in ZDF (n = 6, $P < .05$; Figure S3A). This slight inhibitory effect may involve off-target inhibition of L-type Ca^{2+} channels by SKF.

2.3 | SOCE is reduced in mesenteric arteries of ZDF rats

To directly measure SOCE, isolated SMA smooth muscle cells (SMC) were loaded with the Ca^{2+} dye, fura-2. After store depletion with caffeine (10 mmol/L) in the presence of zero $[Ca^{2+}]_o$, extracellular Ca^{2+} was re-administered in the presence of inhibitors of SR Ca^{2+} ATPase and LTCCs (thapsigargin (TG) 10 µmol/L, and Nif 1 µmol/L, respectively). The resulting increase in intracellular Ca^{2+} can be used as a measure of SOCE. In SMCs obtained from ZL, an instant increase in $[Ca^{2+}]_i$ was observed (Figure 3A). In sharp contrast, the increase was substantially less pronounced in ZDF SMCs, as revealed by comparing the mean change in $[Ca^{2+}]_i$ between ZL (0.20 ± 0.03 ΔFura-2) and ZDF (0.09 ± 0.02 ΔFura-2) rats ($P < .05$, Figure 3B). Exposure to HG significantly inhibits SOCE in SMCs of non-diabetic ZL animals (to 0.06 ± 0.01, n = 5, $P < .05$, Figure 3B). However, this HG-dependent inhibition was not observed in ZDF SMCs (0.09 ± 0.01, n = 8, P = NS vs ZDF vehicle).

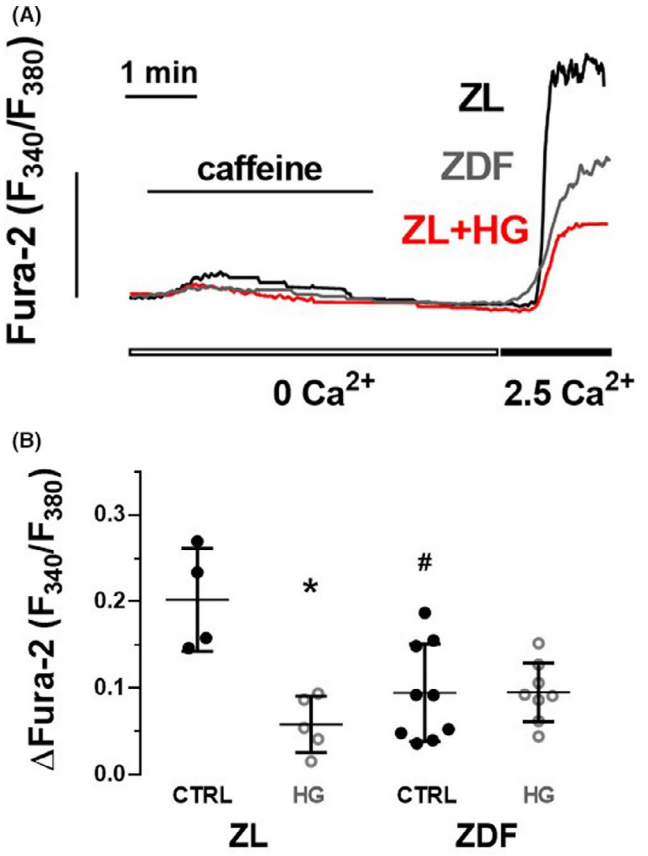

FIGURE 3 Store-operated Ca^{2+} entry (SOCE) is reduced in isolated vascular smooth muscle cells of Zucker diabetic fatty rats (ZDF) rats. A, Representative recordings of $[Ca^{2+}]_i$ measured in FURA-2-loaded, isolated rat vascular smooth muscle cells (VSMCs). Intracellular Ca^{2+} stores were depleted using caffeine (10 mmol/L) in a Ca^{2+}-free solution (0 Ca^{2+}) in the presence of thapisgargin (10 µmol/L) and nifedipine (1 µmol/L). After store depletion and re-administration of 2.5 mmol/L $[Ca^{2+}]_o$, the increase in $[Ca^{2+}]_i$ can be used as a measure of SOCE. B, Scatter plots of quantitative analyses of SOCE amplitude. Compared to Zucker lean (ZL) rats, SOCE amplitude was significantly lower in VSMCs of ZDF rats. Interestingly, compared to vehicle, exposure to high external glucose (HG) resulted in a significant reduction in SOCE amplitude in VSMCs of ZL but not ZDF rats. *$P < .05$ vs corresponding CTRL, #$P < .05$ vs corresponding ZL, two-way ANOVA, n = 4-9 animals

2.4 | Increased Ca^{2+} entry through L-type Ca^{2+} channels partly compensates for reduced SOCE in ZDF animals

As described above, NA-dependent Ca^{2+} release from SR was reduced in SMAs of rats with type 2 diabetes. However, the basal NA-dependent contraction was not different from control (ZL, Figure 1). This suggests that increased trans-sarcolemmal Ca^{2+} entry may compensate for the reduced SR Ca^{2+} release in ZDF. To further investigate the role of LTCC, we measured repetitive NA-dependent contraction of SMAs both at physiologic $[Ca^{2+}]_o$ (2.5 mmol/L) in the presence of nifedipine and also at zero $[Ca^{2+}]_o$. As published previously,[16] Ca^{2+} entry via LTCCs contributes significantly to NA-induced contractions in SMAs, which was also evident from our experiments conducted in the presence of nifedipine and zero $[Ca^{2+}]_o$ (Figure 4). Figure 4B shows that, compared to vehicle, the contraction of SMAs upon NA exposure was significantly diminished in the presence of nifedipine. Importantly, compared to ZL, this impairment of NA-dependent contraction was significantly more pronounced in SMAs of ZDF rats. In the presence of nifedipine, NA-dependent contraction was significantly reduced from 74 ± 4 to 32 ± 4% in ZL but from 75 ± 3 to 19 ± 3% in ZDF SMAs (n = 6, $P < .05$ for ZL + Nif vs ZDF + Nif, Figure 4). The residual NA-dependent contraction observed in the presence of nifedipine may be explained by SOCE. Consistent with direct SOCE measurements, the magnitude of residual NA-dependent contraction in the presence of Nif was significantly smaller in ZDF SMAs compared to ZL (Figure 4). Importantly, additional exposure to HG under the conditions of this assay resulted in a significantly greater inhibition of NA-dependent contractions in SMAs of ZL rats, owing to HG-induced inhibition of SOCE. Consistent with the thesis that SOCE is less influential in diabetic animals, exposure of ZDF rat SMAs to HG had less effect on the magnitude of NA-dependent contractions (Figure 4).

2.5 | Expression of Orai1 is reduced in SMAs of ZDF rats

Stromal interaction molecules (STIM) and ORAI Ca^{2+} release-activated Ca^{2+} modulators (Orai) aggregate to form store-operated Ca^{2+} channels after store depletion.[17] Since we have demonstrated reduced SOCE in SMAs of ZDF rats, we additionally measured the mRNA and protein expression of the STIM and Orai genes (Figure 5 and Figure 6). Table 1 shows the specific primers that were used for measuring mRNA expression.[18] As shown in Figure 5, both STIM1 and two were detected in rat SMAs. Compared to ZL, STIM1 mRNA expression in SMAs of ZDF rats was significantly reduced. However,

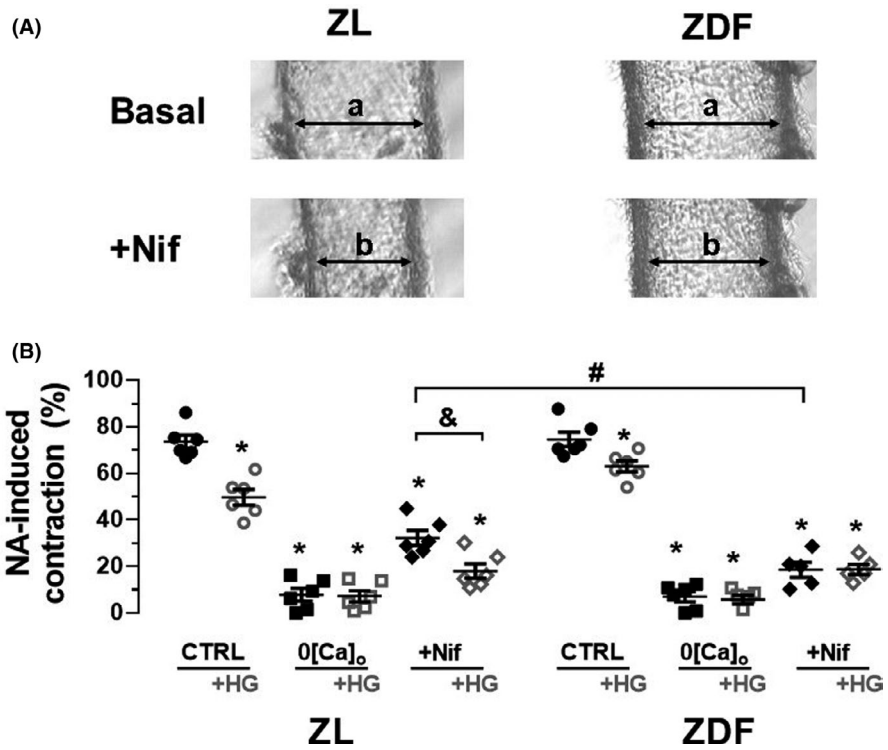

FIGURE 4 After blockade of voltage-operated Ca2+ channels (LTCC), high glucose (HG) inhibits small mesenteric artery (SMA) contraction only in Zucker lean (ZL) but not in Zucker diabetic fatty rats (ZDF). A, Original myographic recordings of SMAs at rest (basal) and after exposure to NA in the presence of nifedipine (Nif, 1 μmol/L, below). Relative NA-induced contractions are shown as scatter plots (B) either upon vehicle, in the absence of external $[Ca^{2+}]$ (0 $[Ca^{2+}]_o$), or in the presence of nifedipine (+Nif). All assays were repeated with exposure to high external glucose levels (HG). Compared to ZL, Nif inhibited NA-induced contraction to a significantly greater extent in the SMAs of ZDF rats, suggesting that Ca^{2+} entry in diabetic SMAs results from a proportionally greater involvement of LTCCs. Moreover, additional exposure to HG (in the presence of nifedipine) significantly reduced NA-induced contraction in ZL, but not in ZDF, mesenteric arteries. $^{*}P < .05$ vs CTRL, $^{\&}P < .05$ vs corresponding CTRL, $^{\#}P < .05$ vs corresponding ZL, two-way ANOVA, n = 5-6 animals

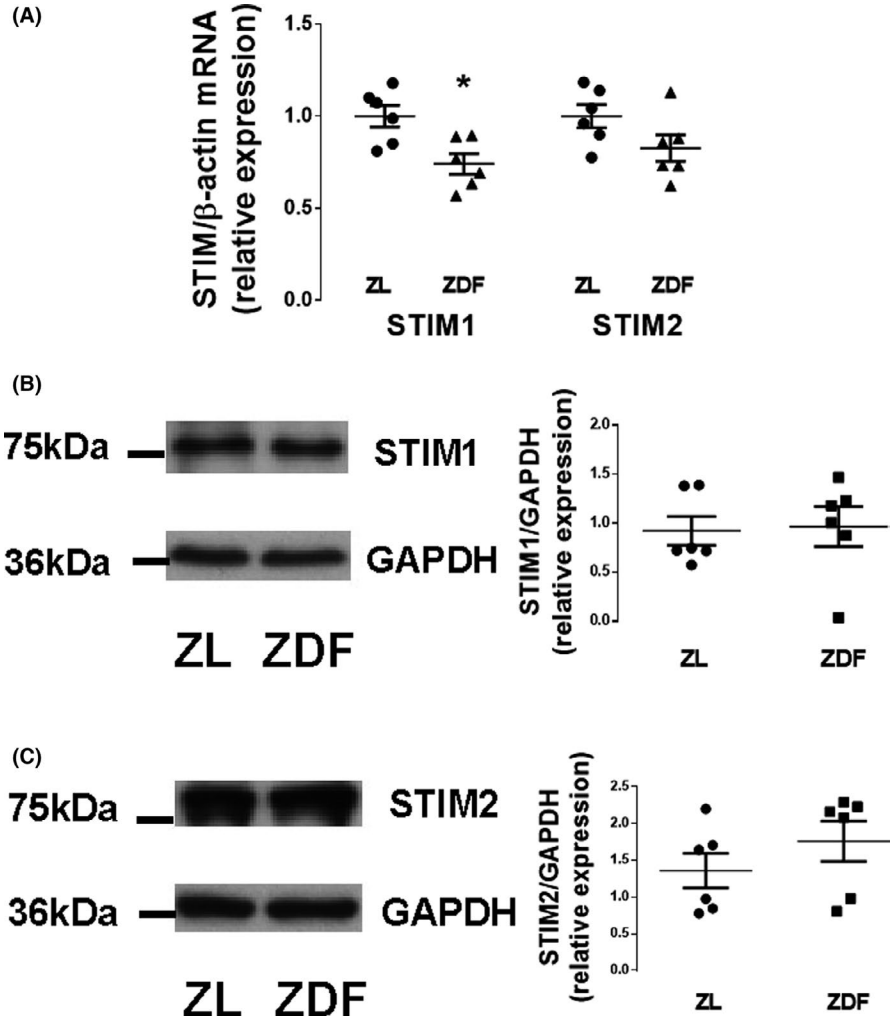

FIGURE 5 Stromal interaction molecule 1 (STIM1) mRNA expression is reduced in Zucker diabetic fatty rats (ZDF) rats. A, Scatter plots of RT-PCR products amplified using primers for STIM1 and STIM2 (relative to β-actin) are shown (see Table 1 for primer details). Compared to Zucker lean rats (ZL), STIM1 mRNA expression in isolated ZDF SMAs was significantly reduced. In contrast, no significant difference in STIM2 expression was detected. Original Western blots and mean densitometric values (normalized to GAPDH) of STIM1 (B) and STIM2 (C) protein expression showing no significant difference between ZL and ZDF. (*P < .05 vs corresponding ZL, n = 6)

protein expression was not different in these groups. Stromal interaction molecules proteins can connect to and functionally interact with TRPC channels.[19] The latter channel proteins are reported to interact with Orai to form heteromeric store-operated Ca^{2+} channels.[20] Measurement of Orai1 revealed reduced protein expression in ZDF, which could account for the reduction in SOCE. Conversely, mRNA expression of Orai and TRP did not significantly differ (Figure 6, Figure S2).

3 | DISCUSSION

Our research shows that intracellular Ca^{2+} handling is severely disturbed in the SMAs from a rat model of type 2 diabetes. Compared to SMAs from non-diabetic lean control rats, intracellular SR Ca^{2+} release in diabetic ZDF rats is reduced in response to the vasoconstrictive agonist NA, which may result from reduced basal SOCE amplitude and reduced NA-dependent stimulation of SOCE. Semiquantitative analyses of protein expression of the ion channel subunits important for SOCE revealed reduced Orai1 expression in ZDF rats. In ZDF SMAs, the lower level of SR Ca^{2+} release was counterbalanced by increased trans-sarcolemmal Ca^{2+} entry via LTCC, resulting in a similar overall magnitude of NA-dependent contraction observed across ZL and ZDF rat models. However, additional exposure to high extracellular glucose levels, which elicits SOCE inhibition, leads to SMA relaxation in ZL, but a dramatically blunted response in ZDF. This finding may have clinical relevance if it translates to the mechanisms underlying cardiovascular complications affecting patients with type 2 diabetes.

3.1 | Diabetic SMAs show reduced NA-dependent SR Ca^{2+} release

It is known that diabetic smooth muscle cells exhibit a severe disturbance of intracellular Ca^{2+} handling.[21] As described above, removal of extracellular Ca^{2+} and blockade of LTCC with nifedipine creates an environment in which NA-dependent transient contractions of SMAs are exclusively dependent upon SR Ca^{2+} release. We show here that SR Ca^{2+} release (measured as NA-dependent contraction) in ZDF SMAs was significantly lower than in ZL SMAs (Figure 2B). This is consistent with previous data collected from a streptozotocin-induced diabetes model.[22,23] In both diabetic murine coronary

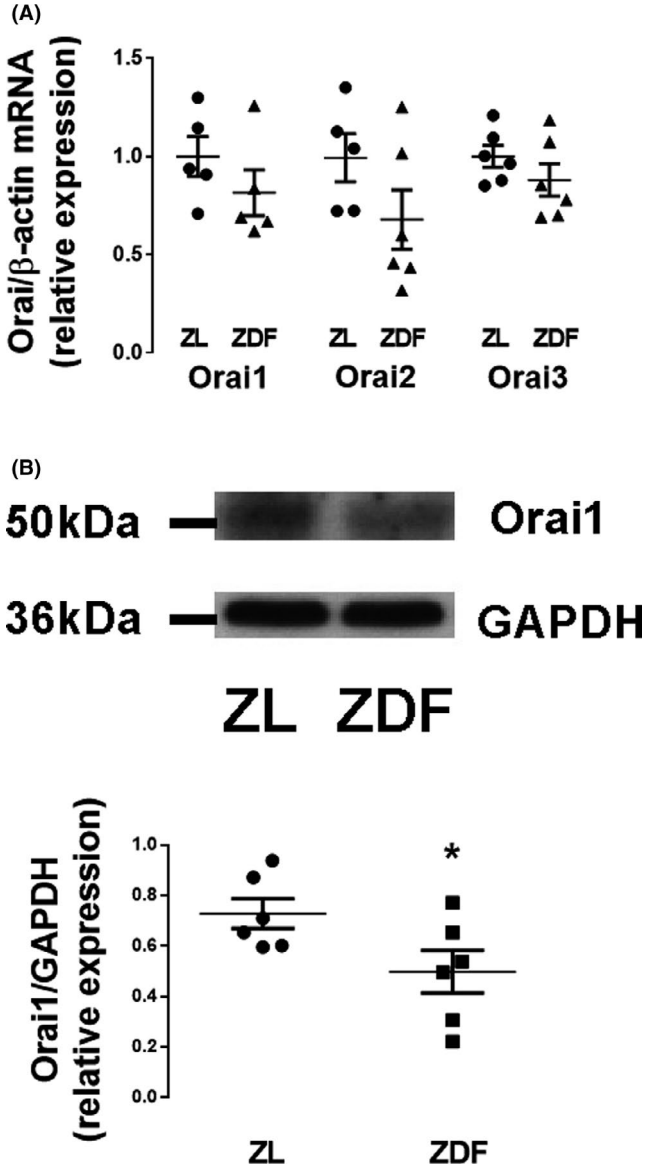

FIGURE 6 Expression of Orai1 is reduced in Zucker diabetic fatty rats (ZDF). A, Scatter plots of RT-PCR products amplified using primers for Orai1, Orai2 and Orai3 (relative to β-actin) in Zucker lean (ZL) and ZDF small mesenteric arteries are shown (see Table 1 for primer details). B, Representative original western blots of Orai1 expression and mean densitometric values (normalized to GAPDH) showing a reduced Orai1 protein expression in ZDF (*$P < .05$ vs ZL)

endothelial cells and diabetic rat aortic smooth muscle cells, a diminished level of store Ca^{2+} release has been reported.[22,23] In accordance, Searls et al report reduced expression of SERCA2/3, as well as IP3-receptor, in type 1 diabetic rat aortae.[24]

3.2 | Diabetic SMAs exhibit reduced SOCE

To elucidate the mechanisms underlying reduced SR Ca^{2+} content and release in diabetic SMAs, we measured store-operated Ca^{2+} entry (SOCE), which is known to regulate SR Ca^{2+} content.[25] While SOCE in SMAs has been previously demonstrated,[5,26] the functional relevance has been unclear. We show here that directly measured SOCE was dramatically reduced in SMCs isolated from the mesenteric arteries of ZDF rats, compared to ZL rats (Figure 3A). Accordingly, the SOCE-dependent tonic contraction of SMAs after re-administration of extracellular Ca^{2+} and LTCC blockade with Nif was also significantly reduced in ZDF compared to ZL animals (Figure 2C).

The relevance of SOCE for artery function in diabetes has been controversially discussed,[27] partly on account of inconsistent data obtained from different species, various models of diabetes, and diverse vascular beds. For example, a reduced SOCE-dependent contraction has been measured in smooth muscle strips isolated from caudal arteries of type 2 diabetic Goto-Kakizaki rats.[28] Reduced SOCE was also observed in SMCs isolated from retinal arterioles[6] and the aorta[23] of a rat streptozocin-induced diabetes model. Conversely, it was shown that SOCE-dependent contraction was increased in saphenous veins isolated from patients with type 2 diabetes.[29] In accordance, increased SOCE has been observed by Kunag et al in renal arteries of type 2 diabetic db/db mice[30] and by Rowghani et al in SMCs isolated from the aorta of rats with streptozocin-induced diabetes,[31] indicating a tissue specific response. Although we cannot explain these incongruities, our data suggest that – at least in SMAs of ZDF rats – SOCE is reduced. This conclusion is further supported by our experiments employing pharmacological SOCE inhibition. Sensitivity to SKF-96365 (SKF) and BTP-2, which are widely used as inhibitors of store-operated Ca^{2+} entry,[32] was less pronounced in SMAs of ZDF rats compared to SMAs of ZL rats (Figure 2A).

Following agonist stimulation and internal Ca^{2+} store depletion, the tonic phase of contraction is elicited by SOCE. This may cause membrane depolarization and coactivate L-type calcium channels to further enhance calcium entry.[33] Importantly, in rat mesenteric arteries, Chen and colleagues have shown that SOCE channels co-localize and activate large-conductance Ca^{2+}-dependent potassium channels (BK_{Ca}).[34] These channels are able to hyperpolarize the membrane potential and thereby reduce agonist-induced contraction.[34] This mechanism potentially prevents excessive contraction of the blood vessels, thereby protecting downstream tissue from undersupply. However, we and others have shown that BK_{Ca} function is reduced in diabetic rat small mesenteric arteries and human vascular smooth muscle,[13,35] suggesting that this protective mechanism may be limited in diabetes. Therefore, in addition to the reduced function and expression of the proteins that facilitate SOCE, impaired BK_{Ca} function may also explain why SMAs from ZDF rats do not relax to the same extent as SMAs from ZL rats in the presence of SOCE inhibitors (after NA-dependent pre-contraction) (Figure 2A).

3.2.1 | What are the mechanisms underlying reduced SOCE in diabetic SMAs?

It is plausible that the level of expression of SOCE-channel subunits has a direct impact on the amplitude of SOCE. STIM is sensitive to Ca^{2+} in

TABLE 1 Oligonucleotide sequences of the inner and outer PCR primers

mRNA	Accession number	Orientation	Primer sequence (5′-3′)	Amplicon
rTRPC1	NM_053558	Forward	CGACACCTTCCACTCGTTCA	254 bp
		Reverse	CGACACCTTCCACTCGTTCA	
rTRPC3	NM_021771	Forward	GCTTGTGTTCAACGCCTCAG	173 bp
		Reverse	ACAGCTCCTTGCACTCAGAC	
rTRPC4	NM_001083115	Forward	ACGCCATCAGGAAAGAGGTG	134 bp
		Reverse	GATAGGCGTGATGTCTGGGG	
rTRPC6	NM_053559	Forward	TGGCAAGTCCAGCATACCTG	182 bp
		Reverse	CTCCGTGTTTCTGCAGAGGT	
rSTIM1	NM_001108496	Forward	TTGTCCATGCAGTCCCCCA	242 bp
		Reverse	AGAGATCCTGGATGGACCCC	
rSTIM2	NM_001105750	Forward	CGACATGTTTGCGAGAACGG	166 bp
		Reverse	CCCGCAATAGGGTAAGGTGG	
rORAI1	NM_001013982	Forward	ACGTCCACAACCTCAACTCC	362 bp
		Reverse	ACTGTCGGTCCGTCTTATGG	
rORAI2	NM_001170403	Forward	CACCTATTTGCCCTGCTCAT	386 bp
		Reverse	AGCTTGTGCAGTTCCTCGAT	
rORAI3	NM_001014024	Forward	GCGGCTACCTCGACCTTATG	246 bp
		Reverse	CCATGAGTGCAAACAGGTGC	
rActb	NM_031144	Forward	CCACCATGTACCCAGGCATT	189 bp
		Reverse	CGGACTCATCGTACTCCTGC	

Abbreviations: Actb, beta-actin; ORAI, Calcium release-activated calcium channel protein; STIM, stromal interaction molecule; TRPC, transient receptor potential canonical.

the SR and activates Orai channels in the plasma membrane if $[Ca^{2+}]_{SR}$ is low. Transient receptor potential (TRP) channels may also be activated by STIM and have been detected in the multimeric proteins forming the Ca^{2+} entry pore.[20] Overexpression of STIM and Orai has been shown to increase SOCE, whereas knockdown of STIM, Orai and TRP has the opposite effect.[36-39] Interestingly, Estrada et al report a downregulation of STIM1 in coronary artery endothelial cells isolated from mice with streptozotocin-induced diabetes.[22] Similarly, reduced STIM1 expression has been found in bladder SMCs of streptozotocin-induced diabetic rats at 12 weeks of age,[40] as well as in embryonic rat cardiomyocytes cultured for 24 hours in HG[41] and in pancreatic beta-cells derived from diabetic patients or streptozotocin-treated mice.[42] Consistent with these data and with the observed reduction of SOCE amplitude in our assays, we show here that STIM1 mRNA expression is reduced in SMAs of ZDF rats, although protein expression in our experiments is comparable to control animals (Figure 5). Moreover, Orai1 protein expression was reduced in our animal model (Figure 6) as seen in tubular cells of patients with diabetic nephropathy,[43] that can account for the reduced SOCE.

3.3 | Diabetic SMAs show increased transsarcolemmal Ca^{2+} entry

Despite reduced SOCE and impaired SR Ca^{2+} release, we show here that SMAs of ZDF rats nevertheless exhibit typical NA-induced contraction under normal conditions (Figure 1). A possible explanation for this observation may be that Ca^{2+} entry via voltage-gated Ca^{2+} channels (LTCC) compensates for the reduced SOCE. To test this hypothesis, we measured the NA-dependent contraction of SMAs in the presence of the LTCC inhibitor nifedipine. We show here that nifedipine inhibited the NA-dependent contraction of SMAs to a significantly larger extent in ZDF compared to ZL rats (Figure 4), which aligns with findings from other groups.[44,45] Navedo and colleagues showed an increased LTCC-dependent Ca^{2+} entry in SMCs isolated from cerebral arteries of mice with type 2 diabetes (db/db). Moreover, they showed that inhibition of PKA equalized the enhanced LTCC activity in db/db mice SMCs.[44] Similarly, it was shown that SMCs from arteries of mice fed with a high-fat diet and from diabetic patients both exhibited increased PKA-dependent LTCC phosphorylation and activity.[45] Interestingly, increased LTCC activity may also result from reduced STIM1 expression. STIM1 has been shown to inhibit LTCC in cortical neurons [46] but this mechanism in diabetic vessels is completely uncharacterized. Reduced SOCE in diabetic SMCs could be partly compensated by LTCC-mediated Ca^{2+} entry. In spite of this, the diminished HG-dependent inhibition of SOCC manifests as impaired vasorelaxation in diabetic SMCs (Figure 7).

3.4 | Increased extracellular glucose inhibits SOCE and impairs contraction

It has been shown that local increases in blood glucose levels lead to vasorelaxation, improved blood flow and consequent increased

perfusion of the intestine, allowing for better motility and transport of nutrition and endocrine factors.[47] The mechanisms that regulate HG-dependent vasorelaxation are not well understood. Exposure to HG was shown to inhibit SOCE in SMCs isolated from the aorta of rats,[48] which is consistent with our data from ZL controls (Figure 3).

Importantly, we were not able to detect this inhibition in SMCs isolated from ZDF rats, which already exhibited dramatically reduced SOCE in the absence of HG. A multitude of diabetic patients suffer from gastrointestinal symptoms,[49] which may be attributed to dysfunction of splanchnic resistance arteries. Furthermore, conditions of HG arise in shock and during stress response.[50] Therefore, we tested the hypothesis that HG-dependent vasorelaxation may be impaired in diabetic SMAs. We show here that exposure to HG completely abolished the NA-dependent, Nif-insensitive contraction of control SMAs (ZL) after Ca^{2+} replenishment (Figure 2C). Since exposure to the SOCE inhibitor, SKF had an almost identical effect on control SMAs (Figure 2), the HG-dependent vascular relaxation (after NA-dependent pre-contraction) may well be mediated by inhibition of SOCE. However, in contrast to control (ZL), HG relaxed NA-precontracted SMAs from ZDF rats to a significantly lesser extent (Figure 1), which is consistent with reduced SOCE in diabetic SMAs. Our data from these animal models suggest that reduced SOCE may underlie the impaired HG-dependent regulation of splanchnic resistance arteries in diabetes.

4 | CONCLUSIONS

Here we show that SOCE is reduced in SMAs of type 2 diabetic ZDF rats, which disturbs contractile function. Conversely, relaxation of diabetic SMAs in response to high glucose levels is impaired, potentially as a consequence of reduced HG-dependent SOCE inhibition. The reduced SOCE amplitude in SMAs of ZDF rats was accompanied by a reduced level of Orai1 protein expression. These results may be instructive for better understanding the intestinal function of patients with diabetes.

5 | METHODS

5.1 | Animals

Equal numbers of male ZDF rats (homozygous for leptin receptor defect, fa/fa) and their respective ZL control rats (heterozygous, fa/+) were procured from Charles River Laboratories (Brussels, Belgium) at the age of 12 weeks. Rats had unlimited access to the diabetogenic diet Purina 5008 (energy rich, containing 26.8% protein, 16.7% fat and 56.4% carbohydrates). Rats were housed in pairs, kept on a 12/12-h light/dark cycle at constant ambient temperature (22–23°C), and had access to food and tap water ad libitum. Animal welfare was assessed every other day on weekdays. At the age of 23–25 weeks, animals were weighed and fasting (6 hours) blood glucose level was assessed at 7 AM: 409 ± 8.3 g and 422 ± 14.5 mg/dL vs 381 ± 9.5 g and 84.7 mg/dL (mean ± SE, n = 10) in ZDF and ZL, respectively. Afterwards, on consecutive weekdays, one rat per day was killed by decapitation following CO_2 overdose in an airtight cage. All animal care and experimental procedures followed German law as well as the Guide for the Care and Use of Laboratory Animals published by the National Institutes of Health, and were approved by the Institutional Review Board at the University of Regensburg.

5.2 | Measurement of mesenteric artery function

Preparation and diameter measurements were performed as previously described.[13] Briefly, SMAs (3rd branch) were dissected

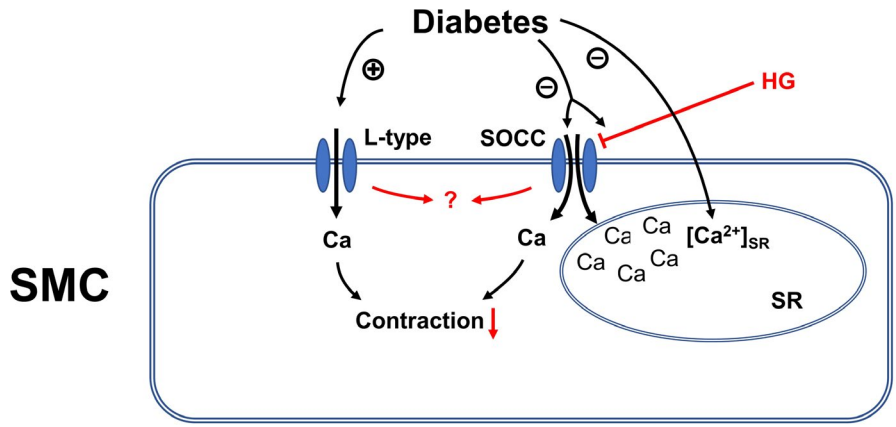

FIGURE 7 Proposed perturbations of Ca^{2+} handling in diabetic small mesenteric arteries (SMAs). In diabetic SMAs, it appears that Ca^{2+} entry through voltage-dependent L-type Ca^{2+} channels is increased, whereas store-operated Ca^{2+} entry is reduced, resulting in a proportionally lower contribution of SOCE to Ca^{2+}-dependent contraction. Exposure of SMAs to high external glucose levels (HG), which occurs naturally during intestinal resorption, inhibits SOCE. This inhibition is accordingly less pronounced in diabetic SMAs, resulting in reduced HG-dependent vasorelaxation. If the findings from these animal models can be replicated in humans, this disruption of Ca^{2+} handling may help to explain the digestive complications experienced by diabetic patients. L-type, voltage-dependent L-type Ca^{2+} channel; SOCC, store-operated Ca^{2+} channel; HG, high glucose; SMC, smooth muscle cell; SR, sarcoplasmic reticulum

and separated from surrounding connective tissue. After mounting vessels between two glass cannulas in a pressure myograph system (Danish Myo Technology model 111P, DMT), vessels were superfused with oxygenated Krebs-Henseleit solution (95% O_2/5% CO_2; constitution in mmol/L: NaCl 118, KH_2PO_4 1.18, KCl 4.7, $MgSO_4$ 1.18, $CaCl_2$ 2.5, D-glucose 5.5, $NaHCO_2$ 25, and EDTA 0.026; pH 7.4 at 37°C). The intraluminal pressure was maintained at 55 mm Hg and the arteries were equilibrated for 40 minutes. After the equilibration period, the resting diameter was measured (Dr), then arteries were stimulated with noradrenaline (NA; 10 µmol/L) to obtain maximal contraction (Dc). This agonist-dependent contraction is mediated by Ca-mobilization from internal stores, increased myofilament Ca-sensitivity and transmembrane Ca^{2+} entry through receptor- and store-operated Ca^{2+} channels.[51] In parallel experiments, contractions were elicited by direct membrane depolarization using high external K^+ (40 mmol/L KCl), which opens L-type Ca^{2+} channels (LTCC).

Endothelial function was examined by superfusion with acetylcholine (ACh, 10 µmol/L). All vessels with intact endothelium used for analysis produced an ACh-induced relative relaxation (R) of >0.7 with R = (Dx-Dc)/(Dr-Dc), where Dx is the actual measured diameter. For some experiments (presented in Figure S1), arteries with denuded endothelia were used. Transient air insufflation eliminated the functional endothelium, and successful denudation was assumed when the ACh-induced relative relaxation was <20%. Experiments were conducted 30 minutes after washout of NA and ACh. For all experiments, relative contraction (C) was calculated according to the following formula: C = (Dr-Dx)/Dr, see also Figure 1. To create an extracellular Ca-free solution (0 $[Ca^{2+}]_o$), $CaCl_2$ was replaced with equimolar $MgCl_2$ and 1 mmol/L EGTA was added to chelate residual Ca. For the 40 mmol/L K^+-containing solution ($40K^+$), NaCl was replaced with equimolar KCl to maintain osmolarity. To minimize subjective bias, rats were investigated in a random order by investigators who were blind to the rat genotype. The same researcher prepared all mesenteric arteries and solutions for myograph experiments. The experiments themselves were conducted by a different researcher who was blind to the experimental group and assay solution.

5.3 | Isolation of smooth muscle cells from SMAs

The VSMCs were isolated as previously described.[52] Briefly, 10 to 15 segments (6–10 mm in length) of SMAs were quickly dissected free of connective tissue in ice-cold Hank's Balanced Salt Solution w/ Ca^{2+} (HBSS1; ThermoFisher, Erlangen, Germany, cat. no. 14025092). Blood and adjacent tissue were removed, and the arteries were placed in the first enzyme solution consisting of Hank's Balanced Salt Solution w/o Ca^{2+} (HBSS2; ThermoFisher, cat. no. 14170112); w/ collagenase type 2 (355 U/mg, ThermoFisher, cat. no. 17101015) for 30 minutes at 37°C to digest the adventitial layer. After allowing the arteries to rest in HBSS1 for 1 minute, remaining adventitia were gently removed mechanically prior to overnight incubation in Dulbecco's Modified Eagle's Medium (DMEM; ThermoFisher, cat. no. 11965-092; w/ 10% (v/v) FBS and w/ 1% (v/v) penicillin-streptomycin solution; penicillin-streptomycin (10 000 U/mL), ThermoFisher, cat. no. 15140122) at 37°C, 5% CO_2. After 24 hours, arteries were cut into sections of approximately 1 mm in length and bathed in the second digestion solution consisting of HBSS2 w/ collagenase (355 U/mg) and elastase type 4 (6 U/mg, Sigma-Aldrich, cat. no. E0258) for 40 minutes at 37°C. After addition of DMEM to arrest digestion, a gentle trituration with a glass Pasteur pipette was performed. Afterwards, the cell suspension was centrifuged at 150 *g* for 5 minutes. Supernatant was aspirated and the cell pellet was resuspended in DMEM. 400 µL of cell suspension was transferred to a laminin-coated glass coverslip and incubated in DMEM for 4 days at 37°C. Experiments were performed by an investigator who was blind to the experimental group.

5.4 | Measurement of intracellular Ca^{2+} handling

Cultured VSMCs derived from ZL or ZDF rats were loaded with Fura-2-AM (in DMEM and 0.02% Pluronic F127) for 30 minutes at room temperature in the dark. Excess Fura-2-AM was then washed out by superfusion for 10 minutes with a Ca^{2+}-free Tyrode's solution containing (in mmol/L) 140 NaCl, 4 KCl, 3.5 $MgCl_2$, 5 HEPES, 1 EGTA, and 10 (vehicle) or 40 glucose (HG) at pH 7.4 (temp 37°C). Thereafter, VSMCs were placed on the stage of an inverted epifluorescence microscope (IonOptix), perfused with Ca^{2+}-free Tyrode's solution and Fura-2 was alternatingly excited at 340/380 nm using a Xenon lamp and Hyperswitch (IonOptix). Fluorescence emission was acquired at 510 nm. For each excitation wavelength, background fluorescence was subtracted and the ratio of the emitted fluorescences F_{340}/F_{380} was calculated as a measure of intracellular $[Ca^{2+}]$. For SOCE measurements, intracellular Ca^{2+} stores were emptied by rapid application of caffeine (10 mmol/L) in the presence of thapsigargin (inhibitor of Ca^{2+} reuptake, TG 10 µmol/L). Thereafter, SOCE was measured by superfusion with Tyrode's solution containing 2.5 mmol/L $[Ca^{2+}]$ in the presence of 10 µmol/L TG and 1 µmol/L LTCC inhibitor nifedipine, as described in.[53]

5.5 | Quantitative RT-PCR

RNA was isolated from first- through third-order branches of small mesenteric arteries of ZL and ZDF rats according to standard procedures. After homogenization of frozen tissue sections (Peqlab), total mRNA was extracted following the manufacturer's directions, with additional DNase digestion to remove all traces of genomic DNA. Total RNA was reverse transcribed into complementary DNA (cDNA), according to standard protocols, as described previously.[4] Briefly, cDNA probes were synthesized in 20 µL reaction volume containing 1 µg total RNA, 0.5 µg oligo(dT) primer (Sigma-Aldrich), 40 U RNasin (Promega, Mannheim, Germany), 0.5 mmol/L dNTP (Amersham), 4 µL transcription buffer, and 200 U Moloney murine leukemia virus RT. No template controls were performed. Real-time quantitative RT-PCR

was performed using an ABI PRISM 7900 detection system (Applied Biosystems) with TaqMan gene expression assays for the genes STIM 1, 2, Orai 1, 2, 3, TRPC 1, 3, 4, 6, together with TaqMan gene expression master mix (Applied Biosystems). Forward and reverse primers were purchased from Biomers and primer sequences are displayed in Table 1. β-actin was used as a reference gene. All water controls and single-stranded RT controls were negative. Data were analyzed using SDS version 2.2.2 software (Applied Biosystems).

5.6 | Western blots

Small mesenteric arteries were isolated, separated from adjunctive tissue, frozen in liquid nitrogen and stored at −80°C. Vessel samples were homogenized in homogenization buffer (12.5 mmol/L sucrose, 0.3 mmol/L NaN_3, 10 mmol/L $NaHCO_3$, pH7, 0.1 mmol/L phenylmethylsulfonyl fluoride, complete protease inhibitors) using TissueRuptor (Cell Signaling Technology), and protein concentration was determined by BCA assay (Pierce Biotechnology). For the immunoblots, the poly (vinylidene difluoride) membrane carrying transferred proteins was incubated at 4°C overnight with anti-STIM1, anti-STIM2 and anti-Orai1 primary antibodies (all 1:200, Sigma [S6072, S8572, AV50117]) or GAPDH control (1:50 000, G8795, Sigma). Immunodetection was enabled using horseradish peroxidase (HRP)–conjugated anti-rabbit or anti-mouse IgG secondary antibodies (1:10 000). Densitometry was performed using ImageJ analysis software, and intensities were normalized to those of GAPDH.

5.7 | Drugs

2-acetoxy-N,N,N-trimethylethanaminium (ACh), (R)-4-(2-Amino-1-hydroxyethyl)-1,2-benzenediol (Norepinephrine, NA), Thapsigargin (TG), D-(+)-Glucose (glucose), DMEM, Ethylene glycol-bis(2-aminoethylether)-N,N,N′,N′-tetraacetic acid (EGTA), Fura-2 pentakis(acetoxymethyl) ester (Fura 2 AM), 4-(2-Hydroxyethyl) piperazine-1-ethanesulfonic acid (HEPES), 1-[2-(4-Methoxyphenyl)-2-[3-(4-methoxyphenyl)propoxy]ethyl]imidazole (SKF-96365), [N-(4-[3,5-bis(Trifluoromethyl)-1H-pyrazol-1-yl]phenyl)-4-methyl-1,2,3-thiadiazole-5-carboxamide] (BTP-2) were purchased from Sigma (Taufkirchen, Germany). Stock solutions were prepared at 10× concentration without glucose, stored at 4°C, and discarded if unused after 14 days. For each day of measurement, fresh solutions were prepared, glucose added, and the pH adjusted to 7.4 at 37°C. ACh, NA and SKF-96365 were dissolved in water; TG and BTP-2 in DMSO.

5.8 | Statistical analysis

Summarized data are reported as mean ± SE. Statistical analysis was performed using GraphPad Prism version 6.0 by blinded investigators. Sample sizes for each experiment were calculated using G*Power (version 3.1.9.2). Experimental results were compared using two-way ANOVA tests to correct for multiple comparisons, except when otherwise stated. *P* values < .05 were considered statistically significant. The number of experiments always refers to the number of individual rats.

ACKNOWLEDGEMENTS

The authors thank G. Pietrzyk and T. Sowa for technical assistance (University Hospital Regensburg, Regensburg, Germany) and B. Jones for editing the manuscript (University of Regensburg, Regensburg, Germany).

CONFLICT OF INTEREST

The authors have no competing interests to declare.

AUTHOR CONTRIBUTION

DE and CS planned the study, FL, MG and CS performed most of the experiments and analyzed/discussed the data together with DE, LM and SW. CS drafted the manuscript, and all co-authors provided critical intellectual input. All authors read and approved the final manuscript.

ETHICS APPROVAL AND CONSENT TO PARTICIPATE, CONSENT FOR PUBLICATION

No patient data were used in this study. All animal care and experimental procedures followed German law and were approved by the Institutional Review Board at the University of Regensburg.

ORCID

Christian Schach https://orcid.org/0000-0001-9560-4015
Stefan Wagner https://orcid.org/0000-0002-9471-1166

REFERENCES

1. Matheus AS, Tannus LR, Cobas RA, Palma CC, Negrato CA, Gomes MB. Impact of diabetes on cardiovascular disease: an update. *Int J Hypertens*. 2013;2013:653789.
2. Roger VL, Go AS, Lloyd-Jones DM, et al. Executive summary: heart disease and stroke statistics–2012 update: a report from the American Heart Association. *Circulation*. 2012;125:188-197.
3. Vanhoutte PM, Shimokawa H, Feletou M, Tang EH. Endothelial dysfunction and vascular disease - a 30th anniversary update. *Acta Physiol (Oxf)*. 2017;219:22-96.
4. Davis MJ, Hill MA. Signaling mechanisms underlying the vascular myogenic response. *Physiol Rev*. 1999;79:387-423.
5. Park KM, Trucillo M, Serban N, Cohen RA, Bolotina VM. Role of iPLA2 and store-operated channels in agonist-induced Ca2+ influx and constriction in cerebral, mesenteric, and carotid arteries. *Am J Physiol Heart Circ Physiol*. 2008;294:H1183-H1187.
6. Curtis TM, Major EH, Trimble ER, Scholfield CN. Diabetes-induced activation of protein kinase C inhibits store-operated Ca^{2+} uptake in rat retinal microvascular smooth muscle. *Diabetologia*. 2003;46:1252-1259.
7. Prakriya M, Lewis RS. Store-operated calcium channels. *Physiol Rev*. 2015;95:1383-1436.
8. Zimmerman MP, Pisarri TE. Bronchial vasodilation evoked by increased lower airway osmolarity in dogs. *J Appl Physiol (1985)*. 2000;88:425-432.

9. MacKenzie A, Cooper EJ, Dowell FJ. Differential effects of glucose on agonist-induced relaxations in human mesenteric and subcutaneous arteries. *Br J Pharmacol*. 2008;153:480-487.
10. Massett MP, Koller A, Kaley G. Hyperosmolality dilates rat skeletal muscle arterioles: role of endothelial KATP channels and daily exercise. *J Appl Physiol*. 2000;89:2227-2234.
11. Ferraris RP, Yasharpour S, Lloyd KC, Mirzayan R, Diamond JM. Luminal glucose concentrations in the gut under normal conditions. *Am J Physiol*. 1990;259:G822-G837.
12. Lu T, Wang XL, He T, et al. Impaired arachidonic acid-mediated activation of large-conductance Ca2 -activated K channels in coronary arterial smooth muscle cells in Zucker diabetic fatty rats. *Diabetes*. 2005;54:2155-2163.
13. Schach C, Resch M, Schmid PM, Riegger GA, Endemann DH. Type 2 diabetes: increased expression and contribution of IK_{Ca} channels to vasodilation in small mesenteric arteries of ZDF rats. *Am J Physiol Heart Circ Physiol*. 2014;307:H1093-H1102.
14. Gangadhariah MH, Dieckmann BW, Lantier L, et al. Cytochrome P450 epoxygenase-derived epoxyeicosatrienoic acids contribute to insulin sensitivity in mice and in humans. *Diabetologia*. 2017;60:1066-1075.
15. Pang Y, Hunton DL, Bounelis P, Marchase RB. Hyperglycemia inhibits capacitative calcium entry and hypertrophy in neonatal cardiomyocytes. *Diabetes*. 2002;51:3461-3467.
16. Wesselman JP, VanBavel E, Pfaffendorf M, Spaan JA. Voltage-operated calcium channels are essential for the myogenic responsiveness of cannulated rat mesenteric small arteries. *J Vasc Res*. 1996;33:32-41.
17. Xu P, Lu J, Li Z, Yu X, Chen L, Xu T. Aggregation of STIM1 underneath the plasma membrane induces clustering of Orai1. *Biochem Biophys Res Commun*. 2006;350:969-976.
18. McDaniel SS, Platoshyn O, Wang J, et al. Capacitative Ca(2+) entry in agonist-induced pulmonary vasoconstriction. *Am J Physiol Lung Cell Mol Physiol*. 2001;280:L870-L880.
19. Ong HL, Cheng KT, Liu X, et al. Dynamic assembly of TRPC1-STIM1-Orai1 ternary complex is involved in store-operated calcium influx. Evidence for similarities in store-operated and calcium release-activated calcium channel components. *J Biol Chem*. 2007;282:9105-9116.
20. Liao Y, Erxleben C, Abramowitz J, et al. Functional interactions among Orai1, TRPCs, and STIM1 suggest a STIM-regulated heteromeric Orai/TRPC model for SOCE/Icrac channels. *Proc Natl Acad Sci USA*. 2008;105:2895-2900.
21. Fernandez-Velasco M, Ruiz-Hurtado G, Gomez AM, Rueda A. Ca(2+) handling alterations and vascular dysfunction in diabetes. *Cell Calcium*. 2014;56:397-407.
22. Estrada IA, Donthamsetty R, Debski P, et al. STIM1 restores coronary endothelial function in type 1 diabetic mice. *Circ Res*. 2012;111:1166-1175.
23. Ma L, Zhu B, Chen X, Liu J, Guan Y, Ren J. Abnormalities of sarcoplasmic reticulum Ca^{2+} mobilization in aortic smooth muscle cells from streptozotocin-induced diabetic rats. *Clin Exp Pharmacol Physiol*. 2008;35:568-573.
24. Searls YM, Loganathan R, Smirnova IV, Stehno-Bittel L. Intracellular Ca2+ regulating proteins in vascular smooth muscle cells are altered with type 1 diabetes due to the direct effects of hyperglycemia. *Cardiovasc Diabetol*. 2010;9:8.
25. Hoth M, Penner R. Depletion of intracellular calcium stores activates a calcium current in mast cells. *Nature*. 1992;355:353-356.
26. Brueggemann LI, Markun DR, Henderson KK, Cribbs LL, Byron KL. Pharmacological and electrophysiological characterization of store-operated currents and capacitative Ca(2+) entry in vascular smooth muscle cells. *J Pharmacol Exp Ther*. 2006;317:488-499.
27. Chaudhari S, Ma R. Store-operated calcium entry and diabetic complications. *Exp Biol Med (Maywood)*. 2016;241:343-352.
28. Mita M, Ito K, Taira K, Nakagawa J, Walsh MP, Shoji M. Attenuation of store-operated Ca^{2+} entry and enhanced expression of TRPC channels in caudal artery smooth muscle from Type 2 diabetic Goto-Kakizaki rats. *Clin Exp Pharmacol Physiol*. 2010;37:670-678.
29. Chung AW, Au Yeung K, Chum E, Okon EB, van Breemen C. Diabetes modulates capacitative calcium entry and expression of transient receptor potential canonical channels in human saphenous vein. *Eur J Pharmacol*. 2009;613:114-118.
30. Kuang SJ, Qian JS, Yang H, et al. The enhancement of TXA2 receptors-mediated contractile response in intrarenal artery dysfunction in type 2 diabetic mice. *Eur J Pharmacol*. 2017;805:93-100.
31. Rowghani S, Emamghoreishi M, Nekooian A, Farjadian S. Enalapril and valsartan improved enhanced CPA-induced aortic contractile response in type 2 diabetic rats by reduction in TRPC4 protein level. *Int J Pharmacol*. 2016;12(8):884-892.
32. Merritt JE, Armstrong WP, Benham CD, et al. SK&F 96365, a novel inhibitor of receptor-mediated calcium entry. *Biochem J*. 1990;271:515-522.
33. Morales S, Camello PJ, Alcon S, Salido GM, Mawe G, Pozo MJ. Coactivation of capacitative calcium entry and L-type calcium channels in guinea pig gallbladder. *Am J Physiol Gastrointest Liver Physiol*. 2004;286:G1090-G1100.
34. Chen M, Li J, Jiang F, et al. Orai1 forms a signal complex with BK_{Ca} channel in mesenteric artery smooth muscle cells. *Physiol Rep*. 2016;4:e12682.
35. Nieves-Cintron M, Syed AU, Buonarati OR, et al. Impaired BK_{Ca} channel function in native vascular smooth muscle from humans with type 2 diabetes. *Sci Rep*. 2017;7:14058.
36. Oh-Hora M, Yamashita M, Hogan PG, et al. Dual functions for the endoplasmic reticulum calcium sensors STIM1 and STIM2 in T cell activation and tolerance. *Nat Immunol*. 2008;9:432-443.
37. Gwozdz T, Dutko-Gwozdz J, Schafer C, Bolotina VM. Overexpression of Orai1 and STIM1 proteins alters regulation of store-operated Ca2+ entry by endogenous mediators. *J Biol Chem*. 2012;287:22865-22872.
38. Kim JY, Zeng W, Kiselyov K, et al. Homer 1 mediates store- and inositol 1,4,5-trisphosphate receptor-dependent translocation and retrieval of TRPC3 to the plasma membrane. *J Biol Chem*. 2006;281:32540-32549.
39. Zhang S, Remillard CV, Fantozzi I, Yuan JX. ATP-induced mitogenesis is mediated by cyclic AMP response element-binding protein-enhanced TRPC4 expression and activity in human pulmonary artery smooth muscle cells. *Am J Physiol Cell Physiol*. 2004;287:C1192-C1201.
40. Yang S, Wang D, Cao X, et al. Store operated calcium channels are associated with diabetic cystopathy in streptozotocininduced diabetic rats. *Mol Med Rep*. 2018;17:6612-6620.
41. Tuncay E, Bitirim CV, Olgar Y, Durak A, Rutter GA, Turan B. Zn(2+)-transporters ZIP7 and ZnT7 play important role in progression of cardiac dysfunction via affecting sarco(endo)plasmic reticulum-mitochondria coupling in hyperglycemic cardiomyocytes. *Mitochondrion*. 2019;44:41-52.
42. Kono T, Tong X, Taleb S, et al. Impaired store-operated calcium entry and STIM1 loss lead to reduced insulin secretion and increased endoplasmic reticulum stress in the diabetic beta-cell. *Diabetes*. 2018;67:2293-2304.
43. Zeng B, Chen GL, Garcia-Vaz E, et al. ORAI channels are critical for receptor-mediated endocytosis of albumin. *Nat Commun*. 2017;8:1920.
44. Navedo MF, Takeda Y, Nieves-Cintron M, Molkentin JD, Santana LF. Elevated Ca2+ sparklet activity during acute hyperglycemia and diabetes in cerebral arterial smooth muscle cells. *Am J Physiol Cell Physiol*. 2010;298:C211-C220.
45. Nystoriak MA, Nieves-Cintron M, Patriarchi T, et al. Ser 1928 phosphorylation by PKA stimulates the L-type Ca2+ channel CaV1.2

and vasoconstriction during acute hyperglycemia and diabetes. *Sci Signal*. 2017;10;eaaf9647.
46. Park CY, Shcheglovitov A, Dolmetsch R. The CRAC channel activator STIM1 binds and inhibits L-type voltage-gated calcium channels. *Science*. 2010;330:101-105.
47. Matheson PJ, Wilson MA, Garrison RN. Regulation of intestinal blood flow. *J Surg Res*. 2000;93:182-196.
48. El-Najjar N, Kulkarni RP, Nader N, Hodeify R, Machaca K. Effects of Hyperglycemia on Vascular Smooth Muscle Ca(2+) Signaling. *Biomed Res Int*. 2017;2017:3691349.
49. Krishnan B, Babu S, Walker J, Walker AB, Pappachan JM. Gastrointestinal complications of diabetes mellitus. *World J Diabetes*. 2013;4:51-63.
50. Marik PE, Bellomo R. Stress hyperglycemia: an essential survival response!. *Crit Care Med*. 2013;41:e93-e94.
51. Mizuno Y, Isotani E, Huang J, Ding H, Stull JT, Kamm KE. Myosin light chain kinase activation and calcium sensitization in smooth muscle in vivo. *Am J Physiol Cell Physiol*. 2008;295:C358-C364.
52. Golovina VA, Blaustein MP. Preparation of primary cultured mesenteric artery smooth muscle cells for fluorescent imaging and physiological studies. *Nat Protoc*. 2006;1:2681-2687.
53. Zhang Y, Wang QL, Zhan YZ, Duan HJ, Cao YJ, He LC. Role of store-operated calcium entry in imperatorin-induced vasodilatation of rat small mesenteric artery. *Eur J Pharmacol*. 2010;647:126-131.

SUPPORTING INFORMATION

Additional supporting information may be found online in the Supporting Information section.

How to cite this article: Schach C, Wester M, Leibl F, et al. Reduced store-operated Ca^{2+} entry impairs mesenteric artery function in response to high external glucose in type 2 diabetic ZDF rats. *Clin Exp Pharmacol Physiol*. 2020;47:1145–1157. https://doi.org/10.1111/1440-1681.13300